Ground-State Guest–Host Chemistry in the Hydrophobic Cavity of the Unsaturated Cyclic $Pd_3(dppm)_3CO^{2+}$ Cluster

Réjean Provencher, Khin T. Aye, Marc Drouin,[1] Jonathan Gagnon, Nicolas Boudreault, and Pierre D. Harvey*

Département de chimie, Université de Sherbrooke, Sherbrooke, Québec, Canada J1K 2R1

Received November 15, 1993®

The guest–host chemistry of the $Pd_3(dppm)_3CO^{2+}$ cluster (dppm = $((C_6H_5)_2P)_2CH_2$) has been investigated in some detail for a series of inorganic and organic substrates by X-ray crystallography (in two cases), UV–visible (and IR) spectroscopy, and molecular mechanics. The two X-ray crystallography characterized complexes are the $[Pd_3(dppm)_3CO](PF_6)_2\cdot(CH_3)_2CO$ and $[Pd_3(dppm)_3CO](CF_3CO_2)(PF_6)\cdot 2(CH_3)_2CO$, which have been used to obtain model structures of the empty cavity (formed by the six upper dppm-phenyl groups) and filled cavity (by the $CF_3CO_2^-$ anion), respectively. The latter was also used as a starting structure for the computations. The binding constants (K_{11}) were measured spectroscopically using the Benesi–Hildebrand (B.–H.), Scatchard (Scat), and Scott (Scot) methods for about 20 different substrates. The stoichiometry of the association is found to be 1:1 where the K_{11} values range from 0.07 to 10 000 M^{-1}. The substrate–cluster associations are competitive and reversible for most studied systems. In some cases (nitro, cyano, and diazonium derivatives), very slow thermal reactions have been observed. Further molecular mechanic calculations on the cluster–aromatic associated complexes showed that agostic interactions are possible at the minimum computed energy configuration for the aromatic compounds. Overall, these studies show that the binding strength of a substrate (both organic and inorganic) into the bifunctional cavity (metallic center and hydrophobic section) is found to be related to a combination of parameters. These properties are the substrate charge and ligand strength, and the size and hydrophobic properties of the substrates. Crystal data: $[Pd_3(dppm)_3CO](PF_6)_2$, 173 K, triclinic ($P\bar{1}$), a = 13.640(4) Å, b = 14.0639(17) Å, c = 22.4835(15) Å, α = 104.291(7)°, β = 105.143(17)°, γ = 99.301(18)°, V = 3914.7(13) Å^3, Z = 2, R = 0.039, R_w = 0.037; $[Pd_3(dppm)_3CO](CF_3CO_2)(PF_6)$, 293 K, monoclinic ($P2_1$), a = 11.0189(10) Å, b = 26.6515(19) Å, c = 14.4746(14) Å, β = 99.786(9)°, V = 4188.9(6) Å^3, Z = 2, R = 0.057, R_w = 0.053.

Introduction

The cluster $Pt_3(dppm)_3CO^{2+}$ is known to be a good catalyst for the water gas shift reaction (WGS),[2] while the palladium analogue acts as a catalyst to the electrochemical CO_2(g) reduction.[3] X-ray crystallographic studies reported by Puddephatt et al. have revealed that the three metal atoms are encircled by a cylindrical array of phenyl rings ("picket-fence-like") forming a cavity.[2,4] The clusters can be considered as bifunctional recognition hosts with a cationic metal center and an hydrophobic cavity. The thermal additions and oxidative additions of substrates into this cavity have been observed exclusively for small molecules.[2a,5] In order to elucidate their thermal and photo-induced oxidative addition reaction mechanisms, we now wish to report the relative competitive binding constants (K_{11}) for selected organic molecules and ions within the cavity of the $Pd_3(dppm)_3CO^{2+}$ cluster in a variety of solvents at 298 K. During the course of this work, the X-ray structures of $[Pt_3(dppm)_3CO](X)(Y)\cdot n(CH_3)_2CO$ (X = Y = PF_6^-, n = 1; X = $CF_3CO_2^-$, Y = PF_6^-, n = 2) were determined to corroborate our binding studies. For the first time the binding ability of the $Pd_3(dppm)_3CO^{2+}$'s cavity is described in some details including the binding of neutral organic molecules.

Experimental Section

Materials. The $[Pd_3(dppm)_3CO]^{2+}$ salts ($CF_3CO_2^-$ and PF_6^-) were prepared according to literature procedures.[4] The mixed salt, $[Pd_3(dppm)_3CO](CF_3CO_2)(PF_6)$, was obtained by multiple partial counteranion metathesis from the CF_3CO_2 salts[4] to the PF_6^- salts (NH_4PF_6). The approximate 50/50 mixture was confirmed by elemental analysis. The solvents dimethylformamide (DMF; Anachemia), acetonitrile (ACN; BDH Co.), dichloromethane (BDH Co.), ethanol (EtOH; Les alcools de commerce Inc.), acetone (BDH Co.), benzene (BDH Co.), toluene (BDH Co.), dimethylacetamide (DMA; Aldrich Chemical Co.), benzonitrile (Aldrich Chemical Co.), nitrobenzene (Anachemia), nitroethane (Aldrich Chemical Co.), methanol (MeOH; BDH Co.), *p*-xylene (Sigma-Aldrich), and triethylamine (Aldrich Chemical Co.) were purified according to standard procedures.[6] The carboxylate salts (sodium benzoate, sodium *p*-methylbenzoate, and sodium *p*-aminobenzoate) were prepared from the neutralization of the corresponding acids (from Aldrich Chemical Co.) by NaOH. The purification was performed from recrystallization in ethanol, and the purity was verified, by ^{1}H-NMR and IR spectroscopy. The sodium acetate (Fisher) and 4-diazo-*N*,*N*-diethylaniline tetrafluoroborate (Aldrich Chemical Co.) were also purified as stated above for the benzoate derivatives.

X-ray structures: $[Pd_3(dppm)_3CO](CF_3CO_2)(PF_6)$. Crystallographic data for $[Pd_3(dppm)_3CO(PF_6)(CF_3CO_2)]\cdot 2(CH_3)_2CO$ at 293 K (Table

* To whom correspondence should be addressed.

® Abstract published in *Advance ACS Abstracts,* July 1, 1994.

(1) Laboratoire de chimie structurale, Université de Sherbrooke.

(2) (a) Puddephatt, R. J.; Manojlovic-Muir, L.; Muir, K. W. *Polyhedron* **1990**, *9*, 2767. (b) Puddephatt, R. J. *Can. Chem. News* **1986**, *36*, 6.

(3) Harvey, P. D.; Mugnier, Y. Unpublished results.

(4) (a) Ferguson, G.; Lloyd, B. R.; Puddephatt, R. J. *Organometallics* **1986**, 344. (b) Manojlovic-Muir, L.; Muir, K. W.; Lloyd, B. R.; Puddephatt, R. J. *J. Chem. Soc., Chem. Commun.* **1983**, 1336.

(5) (a) Rashidi, M.; Puddephatt, R. J. *J. Am. Chem. Soc.* **1986**, *108*, 7111. (b) Douglas, G.; Manojlovic-Muir, L.; Muir, K. W.; Rashidi, M.; Anderson, G. M.; Puddephatt, R. J. *J. Am. Chem. Soc.* **1987**, *109*, 6527. (c) Schoettel, G.; Vittal, J. J.; Puddephatt, R. J. *J. Am. Chem. Soc.* **1990**, *112*, 6400. (d) Ferguson, G.; Lloyd, B. R.; Manojlovic-Muir, L.; Muir, K. W.; Puddephatt, R. J. *Inorg. Chem.* **1986**, *25*, 4190. (e) Jennings, M. C.; Puddephatt, R. J. *Inorg. Chem.* **1988**, *27*, 4280. (f) Lloyd, B. R.; Bradford, A.; Puddephatt, R. J. *Organometallics* **1987**, *6*, 424. (g) Douglas, G.; Jennings, M. C.; Manojlovic-Muir, L.; Muir, K. W.; Puddephatt, R. J. *J. Chem. Soc., Chem. Commun.* **1989**, 159. (h) Bradford, A. M.; Jennings, M. C.; Puddephatt, R. J. *Organometallics* **1989**, *8*, 2367. (i) Manojlovic-Muir, L.; Muir, K. W.; Lloyd, B. R.; Puddephatt, R. J. *J. Chem. Soc., Chem. Commun.* **1985**, 536. (j) Lloyd, B. R.; Manojlovic-Muir, L.; Muir, K. W.; Puddephatt, R. J. *Organometallics* **1993**, *12*, 1231.

(6) (a) Perrin, D. D.; Armarego, W. L. F.; Perrin, D. R. *Purifications of laboratory chemicals*; Pergamon: Oxford, U.K. 1966. (b) Gordon, A. J.; Ford, R. A. *The Chemist's companion, a handbook of practical data, techniques, and references*; Wiley: New York, 1972; p 436.

0020-1669/94/1333-3689$04.50/0

Table 1. Crystallographic Data for $[Pd_3(dppm)_3CO](PF_6)_2 \cdot (CH_3)_2CO$ and $[Pd_3(dppm)_3CO](CF_3CO_2)(PF_6) \cdot 2(CH_3)_2CO$

chem formula	$C_{79}H_{72}F_{12}O_2P_8Pd_3$	$C_{84}H_{78}O_5P_7F_9Pd_3$
fW	1848.47	1874.56
space group	$P\bar{1}$	$P2_1$
T, K	173	293
a, Å	13.640(4)	11.0189(10)
b, Å	14.0639(17)	26.6515(19)
c, Å	22.4835(15)	14.4746(14)
α, deg	104.291(7)	
β, deg	105.143(17)	99.786(9)
γ, deg	99.301(18)	
V, Å	3914.7(13)	4188.9(6)
Z	2	2
λ, Å	0.709 30	0.709 30
ρ_{calcd}, g cm^{-3}	1.568	1.486
μ, cm^{-1}	9.1	8.27
R^a	0.039	0.057
R_w^b	0.037	0.053

^{a} $R = \sum(F_o - F_c)/\sum F_o$. ^{b} $R_w = [\sum w(F_o - F_c)^2/\sum(wF_o^2)]^{1/2}$. $w = (\sigma^2(F) + 0.0002F^2)^{-1}$.

1): dark crystal of dimensions 0.20 × 0.20 × 0.20 mm; M_r = 1874.56; monoclinic; a = 11.0189(10), b = 26.6515(19), c = 14.4746(14) Å; β = 99.786(9)°; V = 4188.9(6) Å^3, space $P2_1$, Z = 2; D_c = 1.486 g cm^{-3}; μ(Mo Kα) = 8.27 cm^{-1}. Data were measured on an Enraf-Nonius CAD-4 diffractometer using Mo Kα radiation (λ = 0.710 73 Å) (graphite monochromated) at a constant speed of 2.7°/min (ω–2θ scan) with $2\theta \leq 44.9°$, hkl range −11 to 11; 0 to 28, and 0 to 15, respectively, and 5608 unique measured reflections. An absorption correction was applied with minimum and maximum transmission factors of 0.8307 and 0.8314, respectively. The structure was solved by direct methods using the NRCVAX system, with atomic scattering factors from Cromer and Waber.[7] The structure was refined using rigid-body substructure for the phenyl rings, for the counteranions PF_6^- and $CF_3CO_2^-$, and for the two solvent molecules. All non-H-atoms were set anisotropic for refinement. Because of the large number of refined parameters, the convergence was achieved after several least-squares refinements using a block-matrix on F, R and R_w being 0.057 and 0.053, respectively, for 3955 observed reflections. The poor quality of the crystal combined with the large thermal motion of the PF_6^- and $CF_3CO_2^-$ anions, as well as the two acetone molecules, prevents a better convergence.

$[Pd_3(dppm)_3CO](PF_6)_2$. Crystallographic data for $[Pd_3(dppm)_3CO](PF_6)_2](CH_3)_2CO$ at 173 K: dark red crystal of dimensions 0.10 × 0.15 × 0.15 mm; M_r = 1848.39; triclinic; a = 13.640(4), b = 14.0639(17), c = 22.4835(16) Å; α = 104.291(7), β = 105.143(17), γ = 99.301(18)°; V = 3914.7(14) Å^3, space group $P\bar{1}$, Z = 2; D_c = 1.575; μ(Mo Kα) = 9.2 cm^{-1}. Data were measured on an Enraf-Nonius CAD-4 diffractometer using Mo Kα radiation (λ = 0.710 73 Å) (graphite monochromated) at a constant speed of 4°/min (ω scan) with $2\theta < 45°$, hkl range −14 to 14, 0 to 15, and −24 to 23, respectively, and 10227 unique measured reflections. An absorption correction was applied with minimum and maximum transmission factors of 0.8119 and 0.8127, respectively. The structure was solved by direct methods using the NRCVAX system, with atomic scattering factors from Cromer and Waber. All non-H-atoms were set anisotropic for refinement.[7]

Spectroscopic Measurements. The absorption spectra were measured on a Hewlett Packard 8452 A diode array spectrometer. The IR spectra were measured on a FT-BOMEM DA 3.002 spectrometer with a resolution of 4 cm^{-1}, typically using from 50 to 256 scans.

Methodology. The linear fit calculations were performed on an IBM 486 PC using the Quatropro program. The competitive binding constants (K_{11}) were measured by plotting $-1/\Delta A$ vs $1/[\text{substrate}]$ (B.–H.), where ΔA is the absorbance change upon the increase in substrate concentration. The ratios intercept/slope in this plot give K_{11}.[8] As a counter check, the K_{11} values have also been evaluated by using the Scat[8] and Scot[8] plots ($-\Delta A/[\text{substrate}]$ vs $-\Delta A$, K_{11} = −slope (Scat); $-[\text{substrate}]/\Delta[A]$ vs [substrate], K_{11} = slope/intercept (Scot)) and are all found to be the same within the experimental uncertainities (±10%) based upon the maximum and minimum values obtained. Typically between eight and fifteen data points were acquired for each measurement which were repeated five to ten times. The solutions were prepared at 295 ± 2 K in the dark, keeping the cluster concentration approximately constant (~2×10^{-5} M) for all experiments. The measurement temperature was not controlled but was monitored (295 ■ 2 K). The change in liquid volumes for the mixing of two different solvents which influences both the $Pd_3(dppm)_3CO^{2+}$ and substrate concentration, potentially inducing systematic errors, was also checked. But in all cases, the variation of volume change was less than 2–3%. In some cases (where the difference is ~3%), the K_{11} values after correcting the ΔA values (based upon the volume change) were calculated and it was found that the K_{11} values did not change more than 3–4%, which is well within the experimental uncertainities. All measurements were performed in the absence of light to ensure that no photochemical process occurs.

The K_{11} values were also measured for the PF_6^- salt on one occasion (acetate/methanol) in order to assert the effect of the counteranion in the competitive binding. $K_{11}(CF_3CO_2^-) < K_{11}(PF_6^-)$ (600 vs 730 M^{-1}), which demonstrates the non-negligible role of the third player $CF_3CO_2^-$. As a consequence, the concentration of $Pd_3(dppm)_3CO^{2+}$ (hence $CF_3CO_2^-$) was kept constant all along this work (~2×10^{-5} M).

Computational Details. The molecular models were built from the crystal structure of $[Pd_3(dppm)_3CO](CF_3CO_2)(PF_6)$, and their energies were minimized using the MAXIMIN force field from SYBYL 5.5 (Tripos Associates, St. Louis, MO). The metal atoms were treated as Pd atoms with a v.d.w. radius of 1.75 Å and charge of +0.667.

Table 2. Selected Bond Lengths and Interatomic Distances (Å)[a]

	$[Pd_3(dppm)_3CO](PF_6)_2$	$[Pd_3(dppm)_3CO](CF_3CO_2)(PF_6)$
Pd(1)–Pd(2)	2.6346(13)	2.610(2)
Pd(1)–Pd(3)	2.5880(13)	2.591(2)
Pd(2)–Pd(3)	2.6166(13)	2.585(2)
Pd(1)–CO	2.0884(7)	2.09(2)
Pd(2)–CO	2.113(7)	2.18(2) 1.99(2)
Pd(3)–CO	2.114(7)	1.97(2) 2.17(2)
Pd(1)–P(1)	2.304(2)	2.327(5)
Pd(1)–P(6)	2.330(2)	2.298(6)
Pd(2)–P(2)	2.348(2)	
Pd(2)–P(3)	2.322(2)	2.300(6)
Pd(3)–P(4)	2.305(2)	2.331(6)
Pd(3)–P(5)	2.298(2)	2.300(5)
C=O	1.159(8)	1.17(2)
Pd(1)···O		2.75(2)
Pd(2)···O		2.68(2)
Pd(3)···O		
Pd(1)–F(8)	4.294(4)	
Pd(1)–F(3)	4.229(4)	
Pd(2)–F(8)	4.313(4)	
Pd(3)–F(5)	4.890(4)	

[a] The atom numbering is included in Figure 3.

Results and Discussion

Structure Descriptions. For the purpose of this work, the crystal structure of $[Pd_3(dppm)_3CO](PF_6)_2$ was examined as it acts as a model compound representing an "empty" cavity. The structural nature of this cavity is now described (Figure 1 and Table 2). Figure 1 shows the cation–anion structure where the PF_6^- anions are located above (unsaturated side) and below (carbonyl-capped side) the Pd_3 plane. At first view, the $Pd_3(dppm)_3$ structure (bond distances and angles) appears normal when compared with the literature data,[2a] but unusual distortions of the Pd_3P_6 plane are observed. Indeed, five of the six P atoms are located above the unsaturated plane with distances for which three of them (P(2), P(4) and P(6)) are unusually moved upward.[10] The other

(7) (a) Larson, A. C. *Acta Crystallogr.* **1967**, *23*, 664. (b) Gabe, E. J.; LePage, Y.; Charland, J.-P.; Lee, F. L. NRCVAX. An Interactive Program System for Structure Analysis. *J. Appl. Crystallogr.* **1989**, *22*, 384. (c) Cromer, D. R.; Waber, J. T. *In International Tables for X-Ray Crystallography*; Ibers, J. A., Hamilton, W. C., Eds.; Kynoch Press: *Birmingham*, England, 1974; Vol. IV, Table 2.2B, pp 99–101 (present distributor: Kluwer Academic Publishers, Dordecht, The Netherlands). (d) LePage, Y. *J. Appl. Crystallogr.* **1988**, *21*, 983. (e) Johnson, C. K. *ORTEP. A Fortran Thermal Ellipsoid Plot Program*; Technical Report ORNL-5138; Oak Ridge National Laboratory: Oak Ride, TN, 1976.

(8) Connors, K. A. *Binding Constants: The Measurements of Molecular Complex Stability*; J. Wiley & Sons: New York, 1987.

(9) Clark, M.; Cramer, R. D., III; Van Opdenbosch, N. *J. Comput. Chem.* **1989**, *10*, 982.

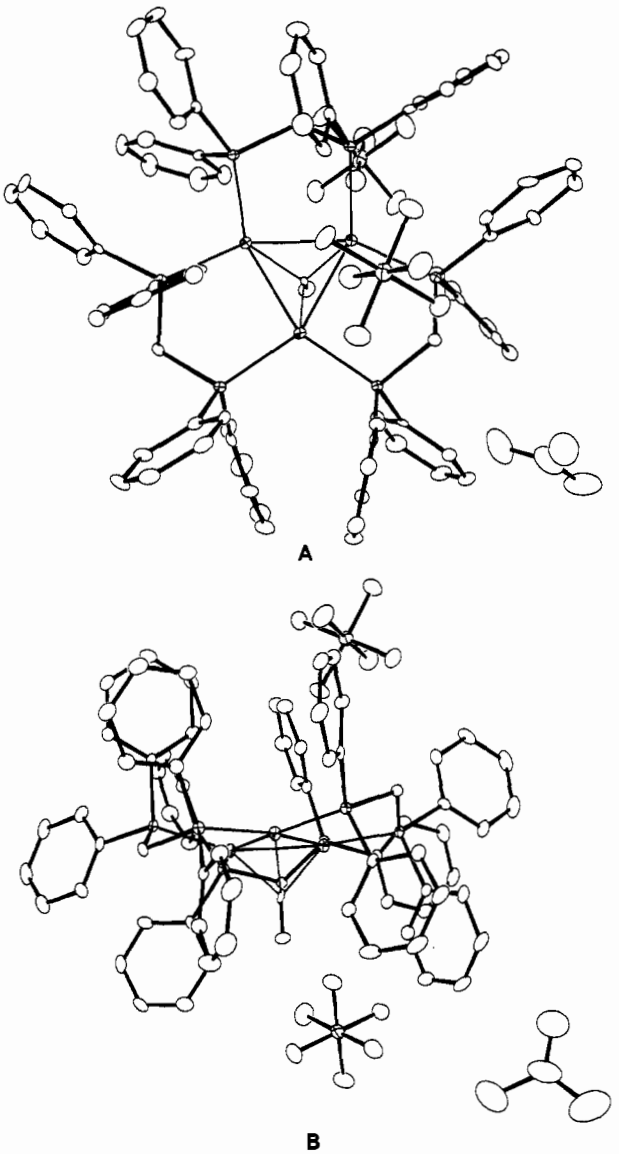

Figure 1. ORTEP views[7e] of $[Pd_3(dppm)_3CO]PF_6)_2 \cdot (CH_3)_2CO$: A = upper view; B = side view. The atoms are shown with 30% probability, and the hydrogens are omitted for clarity.

important features observed are that the cavity (unsaturated side) is indeed found to be "empty" as the closest Pd···F separations are 4.294(4) (Pd(1)–F(8)) and 4.313(4) Å (Pd(2)–F(8)), that the PF_6^- ion does not lie perfectly perpendicular over the Pd_3 plane, but rather it is slid over one of the Pd_2P_2C rings, and that the dppm conformations are different from what was reported so far for the $M_3(dppm)_3$ complexes (M = Pd, Pt).[2a] Normally, the cavity is described by six phenyl groups lying above the M_3P_6 "quasi plane". Exceptionally, only five phenyl rings describe the cavity in this case. All these features clearly appear to be a consequence associated with the absence of a substrate in the cavity. The long Pd–F distances confirm the absence of any Pd···F interactions, but still PF_6^- lies above the entrance of the funnel-shaped cavity. The closest F···C distances are F(9)–C(23) (3.280 Å), F(9)–C(24) (3.267 Å), F(7)–C(24) (3.376 Å), F(8)–C(24) (3.480 Å), F(8)–C(66) (3.345 Å), F(10)–C(14) (3.215 Å), and F(10)–C(15) (3.2205 Å), averaging 3.31 Å, which was essentially equal to the sum of the van der Waals radii (3.15–3.30 Å).[11] The second PF_6^- ion, which is placed on the carbonyl side of the Pd_3 face, lies between the carbonyl and two phenyl groups.

(10) The equation for the Pd_3 plane is given by $-4.723(4)x - 1.634(4)y + 22.2443(10)z = 0.871(4)$. The P···plane distances are P(1) = –0.0189(23), P(4) = –0.6310(22), P(5) = 0.1178(22), and P(6) = –0.5134(22) Å.

Table 3. Comparison of the H···H Distances Describing the Cavities

$[Pd_3(dppm)_3CO](CF_3CO_2)(PF_6)$		$[Pd_3(dppm)_3CO](PF_6)_2$	
H no., H no.	*d*, Å	H no., H no.	*d*, Å
1, 8	2.8	1, 2	2.6
1, 2	2.9	2, 3	2.9
2, 4	3.8	3, 4	3.8
2, 3	2.2	4, 5	2.9
4, 5	3.0	5, 1	3.4
5, 7	4.5		
6, 7	2.1		
7, 8	2.6		
2, 7	6.5	1, 3	5.0
1, 4	5.8	1, 4	4.7
5, 8	5.4	2, 4	4.6

[a] The numbering refers to Figure 4.

Interestingly, the shortest Pd–F distance (Pd(1)–F(3) = 4.229 Å) is similar to that found for the second PF_6^- ion, and the F···C distances are also in the 3.3-Å range. Figure 2 shows a stereoview of the crystal packing. The presence of the PF_6^- ion at the entrance of the cavity appears as a normal consequence of molecular stacking. The presence of the "better binder" acetone molecule outside the cavity (see text below) can only be explained by the electrostatic effects between the Pd_3^{2+} center and PF_6^-, driving the PF_6^- ion as close as possible to the cation blocking the access of the acetone molecule to the cavity. In solution this effect will be significantly diminished due to solvation and dilution effect (see next section.).

The crystal structure of $[Pd_3(dppm)_3CO](CF_3CO_2)(PF_6)$ has also been determined in order to demonstrate the selective binding ability of $CF_3CO_2^-$ over PF_6^-. As expected, the $CF_3CO_2^-$ is found inside the cavity (Figure 3) with Pd···O separations that are indicative of strong electrostatic interactions, i.e. ionic bonding (Pd(1)–O(2) = 2.75(2), Pd(2)–O(3) = 2.68(2), Pd(3)–O(2) = 3.06(2) Å). The Pd···O data compare favorably with those obtained for $[Pd_3(dppm)_3CO](CF_3CO_2)_2$ (2.83, 2.77, 2.92 Å).[2a] The dppm conformation behaves normally, where the six phenyl groups describe the cavity and where four of them lie on one side (axial) and two on the other side (Figure 4) (equatorial). The separations between the ortho-hydrogens are listed in Table 3 for both complexes. In the filled "cavity" two of the methylene groups are exposed and contribute to the description of the cavity: they are numbered from 1 to 8 in Figure 4. The H-atoms of the phenyl groups are more or less at the same distance from the plane describing the Pd_3 center, which make the cavity rather symmetrical. On the other hand, this relationship does not exist for the empty cavity (Figure 4). Although the neighboring H···H separations in the inner portion of the cavity are similar for the "filled" and "empty" cavity (Table 3), the fact that there are fewer members in the "empty" cavity makes the cavity size much smaller (see H···H cross distances in Table 3).

In brief the $[Pd_3(dppm)_3CO](PF_6)_2$ structure exhibits a funnel-shaped opening of about 2.6–3.0 Å in size, in which the five phenyl groups of the dppm adopt a conformation that is less symmetrical than the $[Pd_3(dppm)_3CO](CF_3CO_2)(PF_6)$ one, as though they would have collapsed inward in the absence of substrate. More importantly, the analysis of the dppm conformations clearly indicates the ability of the cavity to change size and shape. Three questions arise: (1) What is the cavity's largest dimension that can adapt? (2) What are the important parameters that drive the binding ability of the cavity (beside the substrate sizes)? (3) What type of trajectory must the substrates adopt during the binding process? The following sections attempt to answer these questions.

Binding Constant Measurements. The binding of substrates into the cavity is accompanied with spectroscopic changes,[5i] where

(11) Huheey, J. *Inorganic Chemistry: Principles of Structure and Reactivity*, 3rd ed.; Harper & Row: New York, 1983; pp 257, 382–86.

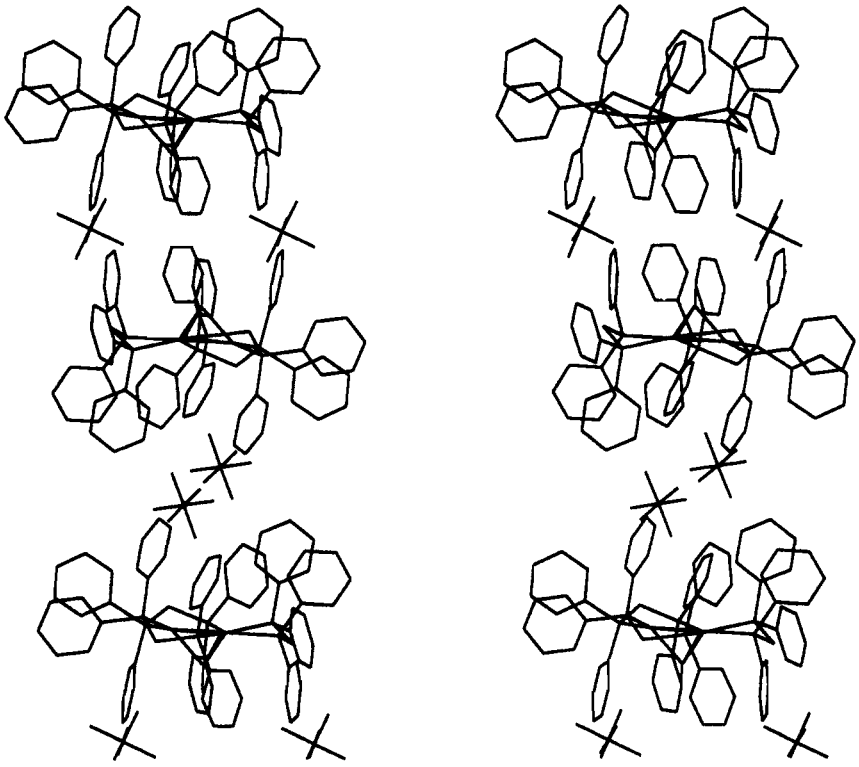

Figure 2. Stereoview of the $[Pd_3(dppm)_3CO](PF_6)_2 \cdot (CH_3)_2CO$ crystal showing the PF_6 anions (octahedral structures) packing outside the cavity of the cluster.

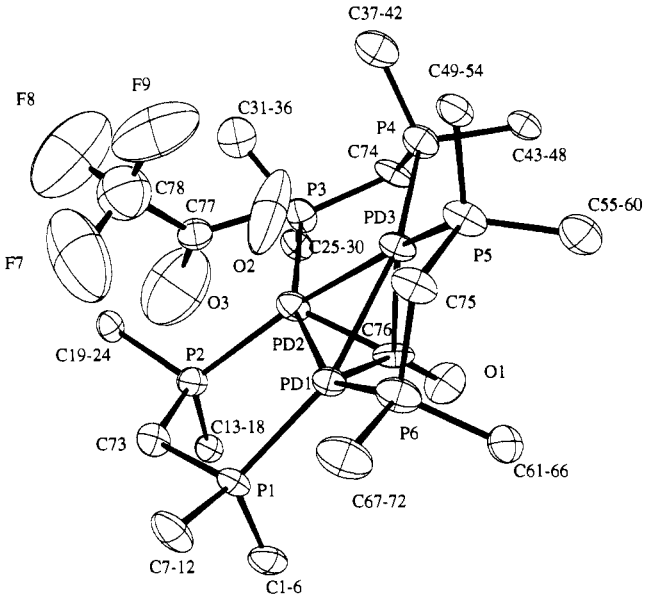

Figure 3. ORTEP view[7e] of $[Pd_3(dppm)_3CO](CF_3CO_2)(PF_6) \cdot 2(CH_3)_2CO$ with 30% probability. The hydrogens and the PF_6^- ion are omitted for clarity.

isosbestic points are evident in the UV–visible spectra. Recently, the λ_{max} of absorption has been reported to be sensitively dependent upon the nature of the substrate including neutral solvent molecules.[12] The solid-state UV–vis spectra (KBr pellets) for the crystallographically characterized $Pd_3(dppm)_3CO^{2+}$ salts, $CF_3CO_2^-$ (filled cavity) and PF_6^- (empty cavity), exhibit very different λ_{max} of absorption values, where the lowest energy band ($e \rightarrow a_2$)[12] is located at 466 and 494 nm, respectively. In this work, the binding constant measurements were performed using Benesi–Hildebrand methodology[8] for complex systems assuming 1:1 stoichiometry as suggested by the X-ray results. In most occasions, the binding constants were also measured using Scatchard and Scott's plots to confirm the stoichiometry.[8] Methanol was used as solvent as the λ_{max} of absorption was the most different (the most red shifted i.e. $\lambda_{max} = 496$ nm) from the others, for cluster and substrate solubility purposes (and for its relatively weak binding ability as the λ_{max} value is essentially identical to the solid-state $[Pd_3(dppm)_3CO](PF_6)_2$ datum). The substrates are divided into two categories: (1) ionic and (2) neutral. For the ionic species, the anionic PF_6^- and a series of carboxylates and the cationic 4-diazo-*N*,*N*-diethylaniline (tetrafluoroborate) salt were used. Typically the concentration in $Pd_3(dppm)_3CO^{2+}$ was kept constant ($\sim 2 \times 10^{-5}$ M) and the $CF_3CO_2^-$ salt was used in all experiments. Upon addition of carboxylate salt into a $Pd_3(dppm)_3CO^{2+}$ methanol solution, spectroscopic changes are observed where isosbestic points are evident. A typical example is shown in Figure 5. In all cases the Benesi–Hildebrand (B.–H.), Scatchard (Scat), and Scott (Scot) plots show linearity with correlation coefficient (σ) larger than 0.98 using 8–15 data points (indicating the presence of a 1:1 association complex). The binding constants (K_{11}) were the same in all cases (B.–H.; Scat; Scot) within the experimental error (10%). Table 4 compares the results, and the data are now interpreted in a systematic fashion.

Carboxylate Compounds. The K_{11} values for these compounds are the largest measured in this work. According to X-ray data the $-CO_2^-$ group points down in the cavity. Further there is no spectroscopic evidence (^{1}H-NMR) for substrates with the R group such as CH_3 or CH_2CH_3 pointing down in the cavity. These experiments demonstrate the presence of two species in equilibrium (and competition). According to the results for the acetate and propionate anion (Table 4), the larger K_{11} for the propionate is consistent with an ionic model for the binding as the greater inductive effect of the ethyl group increases the basicity of the ligand. In this particular case, additional experiments were attempted using ν(C=O) as a spectroscopic probe. The IR data for solid $[Pd_3(dppm)_3(CO)](CF_3CO_2)_2$ and $[Pd_3(dppm)_3CO]^{2+}$ in pure toluene and in toluene containing an excess of CH_3CO_2-Na are as follows; ν(CO) = 1915, 1960 and 1916, 1960 cm^{-1}, respectively. The intensity ratio of the 1916 and 1960 cm^{-1} bands

(12) Provencher, R.; Harvey, P. D. *Inorg. Chem.* **1993**, *32*, 61.

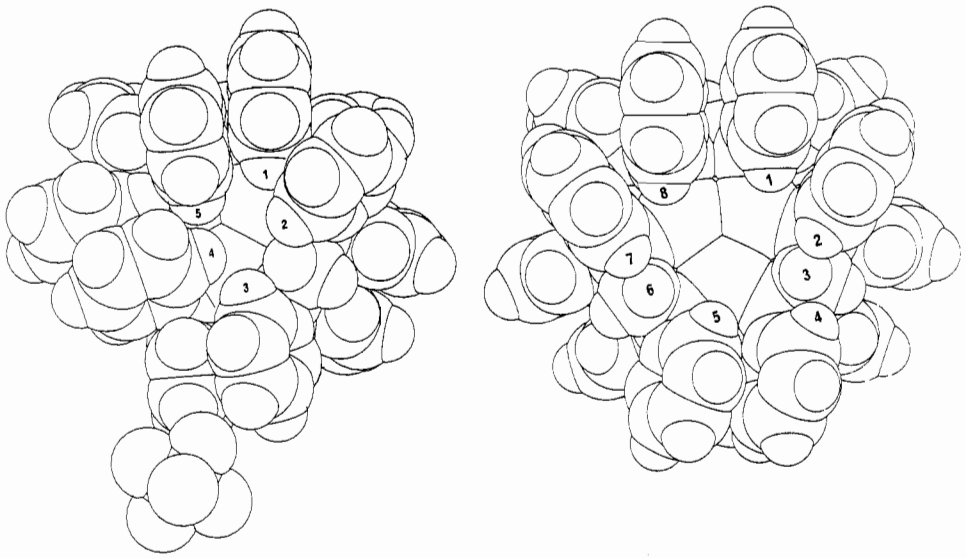

Figure 4. CPK models for $[Pd_3(dppm)_3CO](PF_6)_2$ (A), showing the dppm conformation of the empty cavity, and for $[Pd_3(dppm)_3CO](CF_3CO_2)(PF_6)$ (B), where the $CF_3CO_2^-$ anion found in the cavity is not drawn. Note that the hydrogen atoms are also not represented in the second model (B). The numbering refers to Table 3.

Table 4. K_{11} Values for Various Substrate–$Pd_3(dppm)_3CO^{2+}$ Complexes in MeOH at 298 K

complex with $Pd_3(dppm)_3CO^{2+}$	K_{11}
benzoate	10000 ± 1000
p-toluate	9800 ± 1000
4-aminobenzoate	3300 ± 300
propionate	2600 ± 200
acetate	730 ± 30
4-diazo-*N*,*N*-diethylaniline	(200 ± 100)[b]
nitrobenzene	1.75 ± 0.15
benzonitrile	1.35 ± 0.20
DMF	0.54 ± 0.04
nitroethane	0.17 ± 0.05
acetonitrile	0.10 ± 0.01
toluene	0.08 ± 0.02
p-xylene	0.07 ± 0.01
DMA	0.07 ± 0.01
benzene	<0.07
triphenylmethane	<0.07
water	*a*
hexafluorophosphate	*a*
triethylamine	*a*

[a] No spectroscopic changes observed. [b] The large error is associated with the presence of a reaction.

in the latter case is concentration-dependent on CH_3CO_2Na, indicating that the two species (toluene-bonded and $CH_3CO_2^-$-bonded) are in a competitive equilibrium. Due to the limited solubility of CH_3CO_2Na in toluene, the equilibrium was never completely shifted toward the $CH_3CO_2^-$-bonded species. The benzoate derivatives are interesting as the K_{11} values jump 1 order of magnitude greater. The inductive effect cannot account for this increase, and intermolecular phenyl–phenyl interactions could be at the origin of this phenomena which would bring support to the hydrophobic behavior of the cavity. The surprising result is found for aniline derivative where K_{11} is a third of the one found for the benzene and toluene carboxylate derivatives (Table 4). The inductive effect would argue in favor for an increase in K_{11}, but the hydrophobic properties of the cavity would decrease the ability of the substrate to penetrate deeply into the cavity. This point is discussed further below.

PF_6^- Anion. Excess addition of PF_6^- anions (NH_4^+ salt) into methanol, ethanol, or DMF solutions of $Pd_3(dppm)_3CO^{2+}$ did not lead to any spectroscopic change (until the saturation point), suggesting that the PF_6^- anions do not strongly bind the cavity (in competition with the solvent conditions). The X-ray data for $[Pd_3(dppm)_3CO](CF_3CO_2)(PF_6)$ do indeed confirm the much better binding ability of the $CF_3CO_2^-$ substrate over PF_6^-. The globular shape and the weak ability to act as a ligand for PF_6^- appear to be responsible for this nonexistent binding ability.

Neutral Molecules. Before the diazonium salt is discussed, the binding properties of the neutral molecules are now described. Spectroscopic changes and isosbestic points are also observed upon addition of (neutral) substrates to methanolic solutions of $Pd_3(dppm)_3CO^{2+}$, similar to those observed for the carboxylate derivatives. Again it was easily verified that the B.–H., Scot, and Scat plots exhibit linearity as well (Figure 6).

The reversibility of the binding has also been verified in many cases by increasing the concentration of the substrate and then by decreasing it upon the same sequence of additions. The *A* (absorbance) values were found to be the same for a same substrate concentration. On some occasions, incomplete reversibility was observed for the nitrile and nitro substrates.[13] First, the K_{11} values range from 0.03 to 1.75 M^{-1}, which are 3–4 orders of magnitude smaller than those found for the carboxylate derivatives. The size of the constants reflects the fact that these neutral molecules compete much less efficiently against the methanol molecules to occupy the cavity (competitive bindings). The comparison of the nitroethane vs acetate and the nitrobenzene vs benzoate data (Table 4) clearly indicates the great importance of the substrate charge. It is also important to state that the binding with acetate (or trifluoroacetate) is ionic in nature on the basis of the Pd···O distances (average ~2.83 Å) and to mention that the interactions between the soft Pd metals and the harder O atoms greatly reduce the covalent nature of the substrate···metal associations. Interestingly, the increase of 1 order of magnitude going from an alkyl to a phenyl derivative is also observed for the nitro and cyano substrates. It is important to note that the K_{11} value for benzene is one of the smallest one measured in this work. This observation

(13) The $Pd_3(dppm)_3CO^{2+}$ cluster is found to be slightly unstable in the presence of the cyano and nitro derivatives. For the experimental conditions used in this work (T = 298K, 10^{-1} < [substrate] < 1 M), the variation of the absorbance was less than a few per cent for a 1-h period. The experimental error associated with this behavior is much less than the overall uncertainties of the measurements. In one case, acetonitrile, the product of the reaction between $Pd_3(dppm)_3CO^{2+}$ and (neat) acetonitrile (at 65 °C) is believed to be $Pd_3(dppm)_3(\mu^3\text{-}NCCH_3)_2^{2+}$. This yellow product is relatively unstable as the CH_3CN molecules are very labile in solutions making the purification and characterization of this product more problematic. No further progress has been made on this topic but is still the subject of an ongoing investigation.

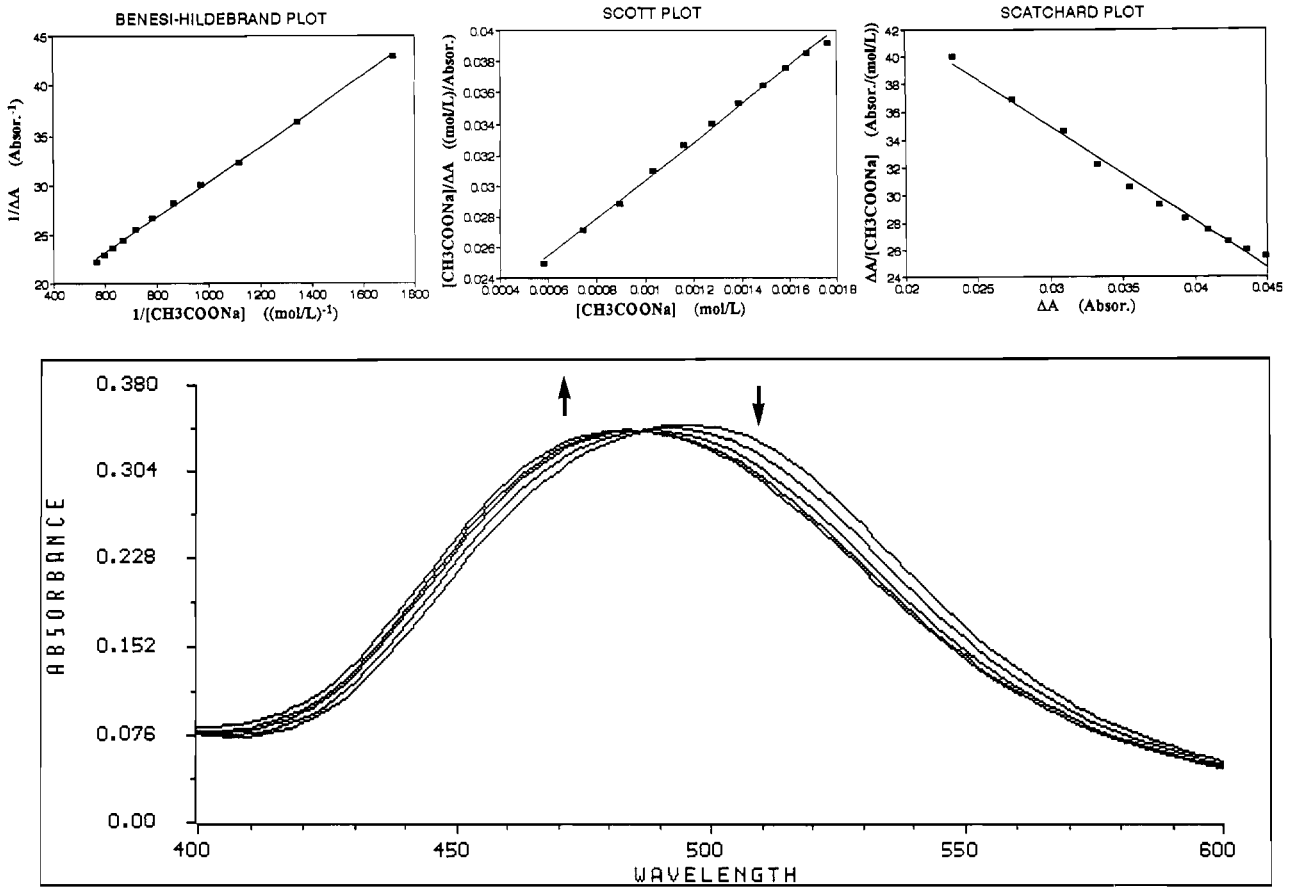

Figure 5. Typical binding constant (K_{11}) measurements experiment for the addition of the acetate ion into a $Pd_3(dppm)_3CO^{2+}$ methanol solution. Only four spectra are shown for clarity. Top: Benesi–Hildebrand, Scott, and Scatchard's associated with the spectra.

clearly indicates the rather very weak binding ability of the phenyl group, which rules out the increase in K_{11} from an alkyl to a phenyl derivative to be associated with an efficient binding via the phenyl group.

The sensitive decrease in K_{11} going from DMF to DMA strongly suggests that the binding of DMF (and DMA) must proceed via C=O···Pd_3 interactions. Additions of triethylamine did not induce any spectroscopic change as discussed for the PF_6^- anion and leads to the conclusion that the binding of DMF (and DMA) does not occur via the $-N(CH_3)_2$ group.

One of the important experiments in the work is the addition of water to the solutions, asserting the hydrophobic properties of the cavity. First, $Pd_3(dppm)_3CO^{2+}$ is water insoluble. Dilution experiments were performed in various solvents (additions of pure water to solutions of methanol, DMF, and acetone), bearing in mind that the change in concentration of $Pd_3(dppm)_3CO^{2+}$ should be corrected (in the event that K_{11} could be obtained). This was not necessary as the λ_{max} of absorption never changed upon addition of water (up to 80%, v:v) to any of the solutions investigated. Despite the small size of the molecule and the relatively good ability of water to act as a ligand (according to the spectroscopic series),[11] the water molecule just does not penetrate the cavity. Recent studies[14] showed the emission lifetimes (τ_e) of the $Pt_3(dppm)_3CO^{2+}$ compound dissolved in eight different solvents (at 77 K) demonstrating that τ_e was solvent dependent *but not* water dependent (the investigated range of water amount was between 0 and 10% v:v). We also noticed that, for the few systems verified, K_{11} was not water sensitive (within the experimental uncertainties).

Due to the proximity in λ_{max} values for $Pd_3(dppm)_3CO^{2+}$ in a number of solvents, the addition of some solvent/substrates into a $Pd_3(dppm)_3CO^{2+}$ methanol solution did lead to spectroscopic changes with the presence of isosbestic points but the ΔA values were so small that no accurate value for K_{11} could be obtained. Instead, additions of DMF into solutions of $Pd_3(dppm)_3CO^{2+}$ were performed as λ_{max} for DMF solutions were very different from the others (acetone, dichloromethane, methanol, acetonitrile, and toluene). The data are listed in Table 5. Again clear spectrocopic changes and isosbestic points were observed and the B.–H., Scot, and Scat plots exhibit linearity. These systems are also reversible. In this scale a greater K_{11} value (see DMF/toluene) indicates that the DMF molecule (acting as a substrate) competes more efficiently with respect to the solvent, when compared to systems with smaller values (see DMF/acetone). Hence the relative binding strength (taking into accout the experimental uncertainities) varies as acetone ~ dichloromethane < methanol ~ acetonitrile < toluene. On the basis of the DMA/methanol, acetonitrile/methanol, and DMF/methanol results of Table 4, DMF appear to be a better binder than acetone and acetonitrile.

Table 5. K_{11} Values for the DMF–$Pd_3(dppm)_3CO^{2+}$ Complex in Various Solvents at 298 K

solvents	K_{11}[a]	solvents	K_{11}[a]
toluene	0.71	dichloromethane	0.26
acetonitrile	0.45	acetone	0.24
MeOH	0.41		

[a] The experimental uncertainties are ±10%.

Although the data provide direct evidence for the relative binding ability of the $-CO_2-$, $-NO_2$, –CN, and >C=O substituents (and the phenyl group), the binding site in methanol substrate is more problematic. The hydrophobic behavior of the cavity suggests that the penetration of the –OH group should not be favored. The similarity in binding ability for acetonitrile and methanol (Table 5) indicates that the binding of the –OH group must be similar to that of –CN. Intuitively, the relative better

(14) Harvey, P. D.; Hubig, S.; Ziegler, T. *Inorg. Chem.*, following paper in this issue.

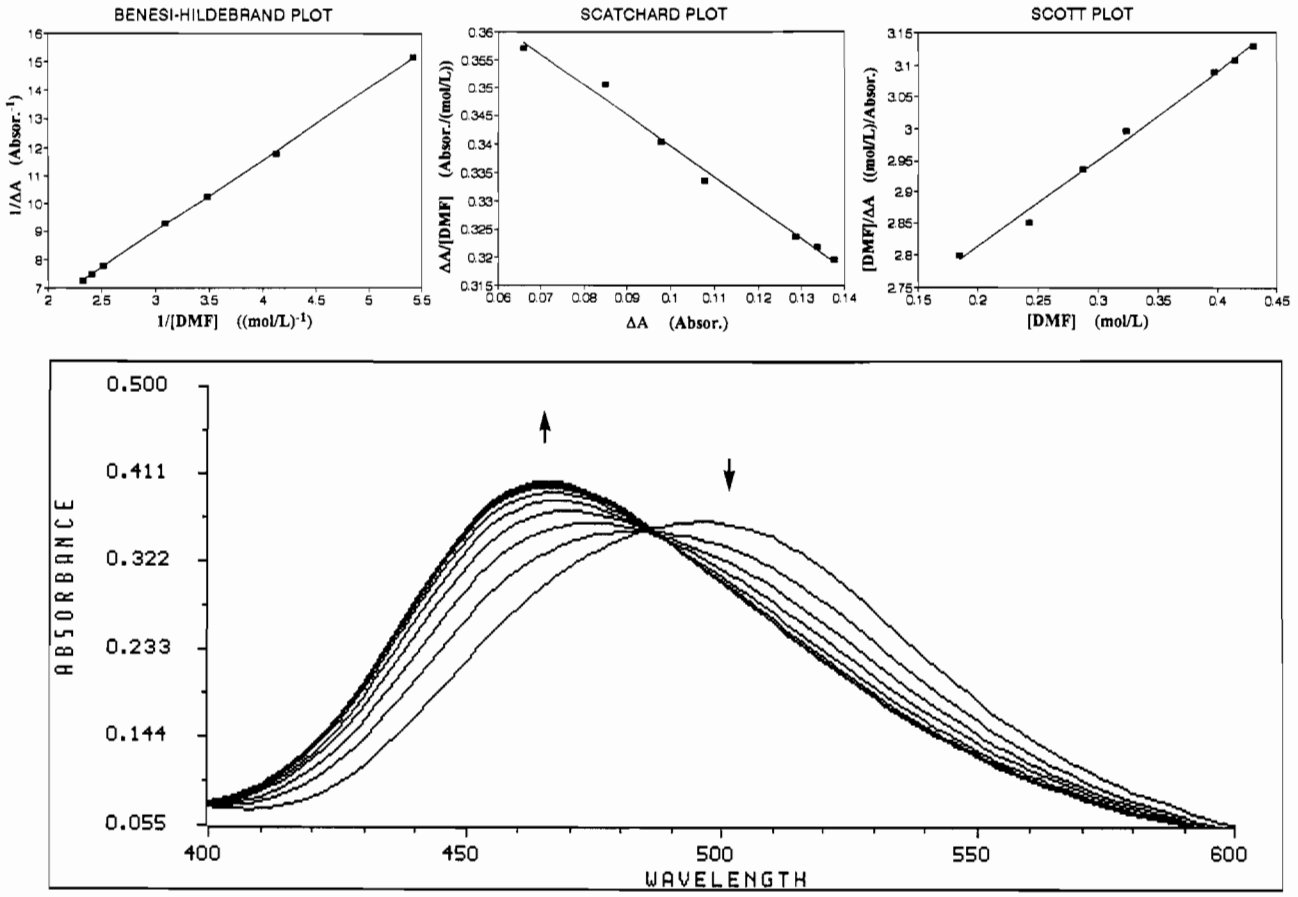

Figure 6. Typical K_{11} measurements experiment for the addition of DMF into a $Pd_3(dppm)_3CO^{2+}$ methanol solution, with the Benesi–Hildebrand, Scatchard, and Scott plots associated with the spectra.

ligand ability of methanol (vs water) via inductive effects (CH_3 vs H) and the lesser H-bonding interactions in the methanol solvent may appear as important factors promoting some evidence for binding with methanol. The use of phenol as substrate appears appropriate to elucidate this point, but the strong ease to dissociate in phenolate and H^+ [15] prevents further consideration of this substrate at this point.

Aromatic Compounds. In order to understand the role of the hydrophobic interactions, particularly involving aryl–aryl contacts, the use of aromatic substrates such as benzene, toluene, *p*-xylene, and triphenylmethane were also investigated. In all cases spectroscopic changes and isosbestic points are observed, with B.–H., Scat, and Scott's plots also exhibiting some linearity ($\sigma > 0.98$). The decrease in linearity in these cases is associated with the size of K_{11}. It appears that the smaller the K_{11} (substrates vs methanol), the more difficult it is to measure where the slopes and intercepts become sensitively more fluctuating from one experiment to another, consequently increasing the experimental uncertainities. The K_{11} values (Table 4) are indeed small as expected from a size point of view but do not appear to be negligible. The important result is the fact that these constants, in most cases, are the smallest ones measured, indicating that the binding is weak. Essentially, the substrates act as guest molecules rather than ligands. The spectroscopic changes could be induced by weak intermolecular agostic interactions (Pd···H–C) as suggested by the modeling experiments described below. The K_{11} values for benzene and triphenylmethane as substrates were not obtained, as the slopes and intercepts were difficult to measure due to the small size of these values. However, the amount of substrates necessary to induce a fixed ΔA value (for substrates where λ_{max} are the same) varies as toluene $\leq$ *p*-xylene < benzene < triphenylmethane. This observation implies that the K_{11} values should vary as toluene $\geq$ *p*-xylene > benzene > triphenylmethane. In Table 4 the data for benzene and triphenylmethane are reported as being $<0.07\ M^{-1}$ (the value measured for *p*-xylene). Because the K_{11} values for toluene and *p*-xylene are the same (within the experimental error) and are qualitatively larger than that of benzene and triphenylmethane, the penetration of the methyl groups appears to be easier than that of the binding of a phenyl group into the cavity. The molecular modeling experiments described below are consistent with these findings.

Diazonium Salt. The use of a diazonium salt was made in order to further investigate the substrate charge effect on K_{11}. The small size of the $N{\equiv}N^+-$ group and the bulky portion of the $(CH_3CH_2)_2N-$ substituent[16] (in the para position) force a unique possibility of binding to occur in the molecular axis with the $N{\equiv}N^+-$ group pointing down in the cavity. Due to the charge, one would expect weak bindings to occur. Sterically, the diazonium salt resembles benzonitrile, which would, in principle, be placed at an upper limit of $1.35 \pm 0.20\ M^{-1}$ (Table 4). Experimentally, an unusually large value was observed ($200 \pm 100\ M^{-1}$). The large uncertainty is related to the presence of a very slow reaction making the system partially irreversible.[17] In order to measure K_{11}, the substrate concentration was kept low in order to slow down the reaction. The disappearance of the

(15) Allinger, M. L.; Cava, M. P.; De Jongh, D. C.; Johnson, C. R.; Lebel, N. A.; Stevens, C. L. *Organic Chemistry*; McGraw-Hill: New York, 1975.

(16) Due to the fact that benzene exhibits weak bindings and the primary assumption that the $N{\equiv}N^+-$ group would be a weak binder (due to the positive charge), the *para*-substituted derivative was chosen in these experiments to prevent any interference from the benzene group. The $(CH_3CH_2)_2N-$ substituent was appropriate in that respect since no binding was observed for triethylamine.

(17) The nature of the product appears to be the $Pd_3(dppm)_3(CO)(L)^{3+}$ compound (L = diazonium compound) on the basis of the preliminary spectroscopic analysis. Unfortunately we have been unable to obtain a crystal suitable for X-ray diffraction analysis. Harvey, P. D.; Socol, S. M. Unpublished results.

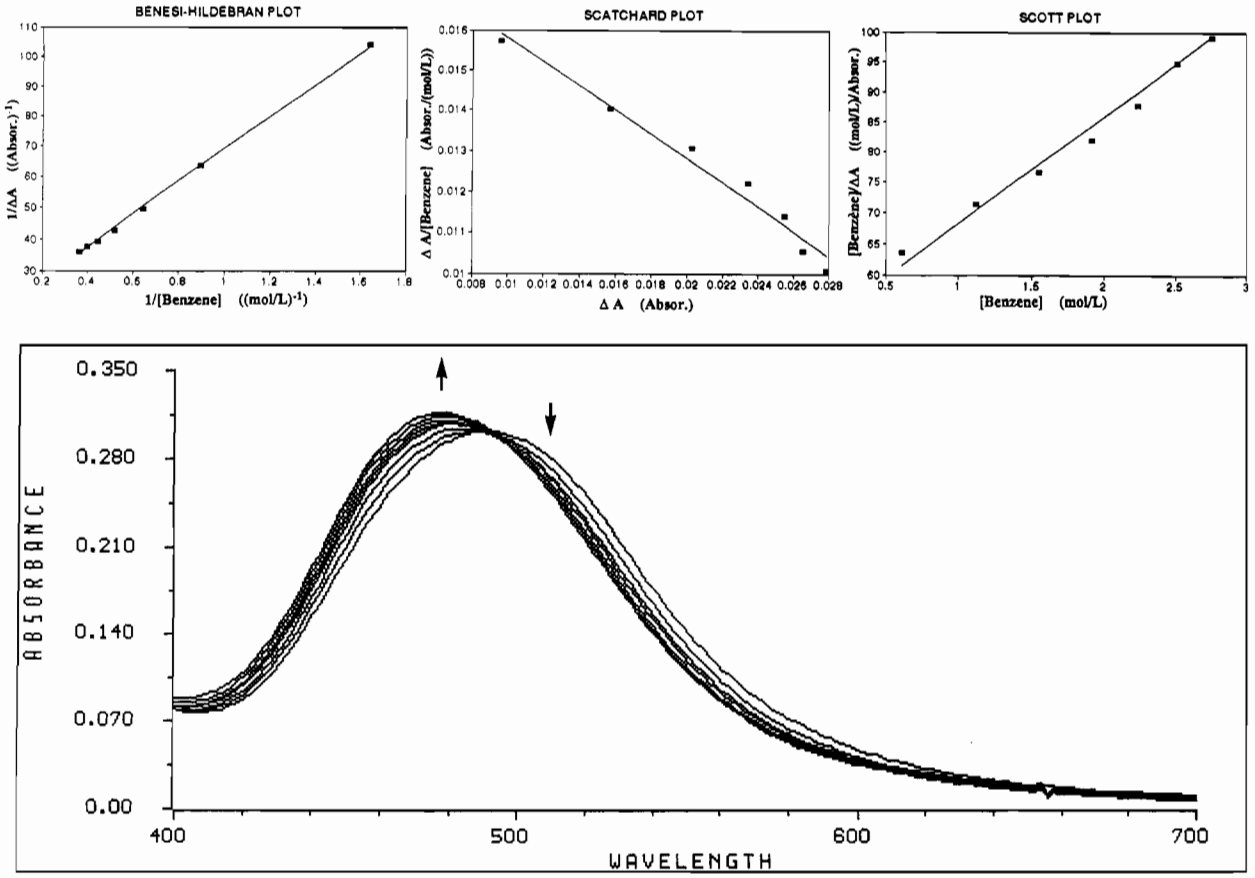

Figure 7. Typical K_{11} measurements experiment for the addition of benzene into a $Pd_3(dppm)_3CO^{2+}$ methanol solution, with the Benesi–Hildebrand, Scatchard, and Scott plots associated with the spectra. Note that the correlation coefficients are at least 0.98 in all three plots.

starting material was monitored as a function of time for $Pd_3(dppm)_3CO^{2+}$ concentrations that were typical for the K_1 measurements, and no more than 2–3% of the total concentration actually reacted during the period of time that was necessary to perform the measurements. Because the concentrations of the substrate were kept low, the evaluation of the intercepts (or the slopes for the various plots) became more difficult. These reported K_{11} values should be considerd as an approximate magnitude for binding rather than an accurate one. Beyond any doubt K_{11}(diazonium) > K_{11}(benzonitrile) and may intuitively reflect the better π-acidity of the diazonium ligand (due to the positive charge). These experiments do not provide information whether the interactions of the N atoms (in the diazonium and benzonitrile substrates) proceed via a triply bridging structure (μ^3-N) or a terminal structure as found in the crystal structure using phosphite and xylyl isocyanide ligand substrates.[18–20] However in a weakly interacting Pd_3···S system, steric arguments strongly favor the μ^3-N binding structure. The ^{1}H-NMR analysis exhibit an AB quartet similar to that of the starting material supporting this hypothesis. These experiments further demonstrate that the ligand properties of a substrate are very important in the binding.

Computer Modeling. The molecular mechanics calculations were used to obtain some insight about the steric interactions between the substrates and the dppm ligands. The computations do not consider any metal–ligand interactions (including agostic interactions) but take into accout the electrostatic and van der Waals effects. Further, they do not take into account the presence of the solvent molecules outside the cavity interacting with part of the substrate (in vacuo), rather they consider only what the cavity (electrostatically and sterically) can do to influence the behavior of the substrates within the cavity when it can be done with some confidence. In the first modeling, the strongly binding carboxylate substrates were considered (particularly the benzoate anion). The X-ray structure for $Pd_3(dppm)_3CO^{2+}$ mixed salt was used (as the structure involves the CO_2^- group in the cavity). In this modeling experiment, the CF_3 group was replaced by a phenyl group prior minimization. After minimization, the benzoate ligand remains planar and adopts a bent configuration (100.2°) with respect to the Pd_3 plane (Figure 8) where the phenyl group of the benzoate lies on phenyl groups no. 1 and no. 8 (the numbering refers to Figure 4). Some dppm phenyl rotations (along the P–C bonds) are to be ~2.8 Å between the ortho-hydrogen of phenyl no. 5 and the closest meta-carbon of the

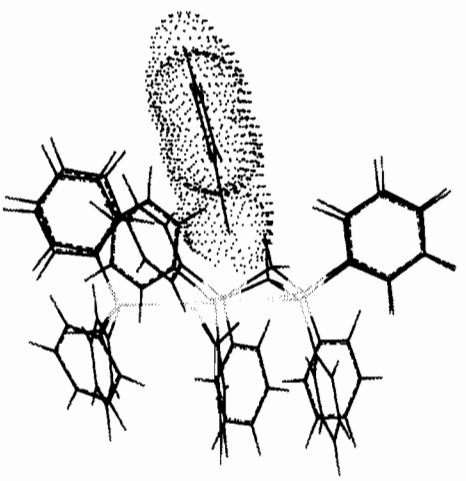

Figure 8. Minimized structure of the associated complex $Pd_3(dppm)_3CO^{2+}$–benzoate ion, where a 2+ charge is set at the Pd_3 center.

(18) Bradford, A.; Jennings, M. C.; Puddephatt, R. J. *Organometallics* **1988**, *7*, 792.
(19) Bradford, A. M.; Douglas, G.; Manojlovic-Muir, L.; Muir, K. W.; Puddephatt, R. J. *Organometallics* **1990**, *9*, 409.
(20) Bradford, A. M.; Payne, N. C.; Puddephatt, R. J.; Yang, D. S.; Marder, T. B. *J. Chem. Soc., Chem. Commun.* **1990**, 1462.

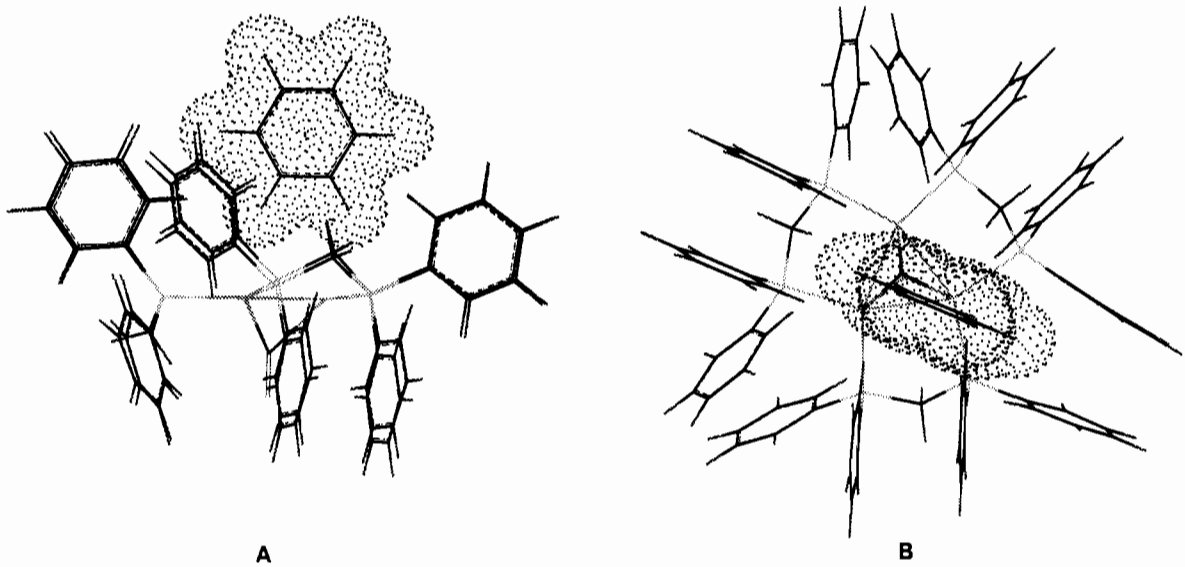

Figure 9. Side (A) and upper (B) view of the cavity filled with a benzene molecule based upon a minimized structure.

benzoate substrate. This distance is essentially equal to the sum of the van der Waals radii.[11] The presence of the methylenes (no. 3 and no. 6) induces some steric hindrance at the bottom of the cavity.

The shortest computed Pd···O distances range from 2.53 to 2.60 Å distances and compare somewhat reasonably to those obtained crystallographically for the $CF_3CO_2^-$ ion (2.68–2.75 Å; Table 2). The most important feature is that the CO_2^- group with respect to the Pd_3 frame adopts a very specific orientation (identical to the X-ray results). The CO_2^- group sits on top of the M_3 center in a C_{2v} symmetry with the Pd–O separations as similar as possible in order to spread the electrostatic interactions as equally as possible. One minor difference between the $CF_3CO_2^-$ (from the X-ray results) and $C_6H_5CO_2^-$ conformations (from the modeling results) occurs and is the Pd_3···substrate molecular axis angle which is 81.4(4)° for $CF_3CO_3^-$ and 79.8° for $C_6H_5CO_2^-$ but in the opposite direction. This minor difference in behavior could be associated with the shortest Pd···O distances in the computational data. From all of these experiments, the electrostatic attractions (Pd_3···^-O_2CR and the phenyl–phenyl interactions) clearly appear to be the main factors that drive both the binding and the favored conformation of the substrate in the cavity.

The modeling experiments for the nitro derivatives have also been performed. No X-ray data are available at this time to set the Pd–O distances, and the relative orientation of the NO_2 group inside the cavity. Structurally speaking the NO_2 group resembles the CO_2^- one. In the different modeling experiments, the NO_2 group was placed inside the cavity similar to the CO_2^- one as shown in Figure 8 and with different orientations of the NO_2 group with respect to the Pd_3 frame. After the computations, the NO_2 substrate moved out of the cavity where one of the two oxygen atoms pointed down in the cavity with a shortest Pd···O approaching 3 Å. Many minimum energy configurations were observed and depended upon how the molecule was set in the cavity prior to minimization. The main conclusion from these experiments is that the charge definitely plays a major role in the substrate binding. Due to the fact that the computations do not take into account the metal–ligand interaction properties, these experiments are inconclusive with respect to the true structural nature of the R–NO_2···Pd_3 binding. At this point, one can only speculate that the –NO_2–Pd_3 coordination and binding can be structurally related to the –CO_2^- one described above.

The structural properties for the cyano derivatives cannot be approached with a unique model as Puddephatt *et al.* showed that the ligand isocyanide was labile over the Pd_3 center (terminal $\rightleftarrows$ μ^3-bridging). As the comment stated for the –NO_2 substrates, any attempt to model these substrates would be unsubstantiated with the program used. In the DMF case, the binding occurs via the carbonyl group which suggests that the –CHO group lies inside the cavity, structurally similar to the carboxylate derivatives, and similar conclusions for the binding geometry are to be expected, particularly when no electrostatic interactions are involved. The very small K_{11} value for the sterically hindered DMA (0.07 M^{-1}) indicates that the nature of the substrate contact with the cavity is somewhat similar to that of benzene (hydrophobic and perhaps agostic interactions; see text below). Because of the multitude (weak) binding sites (three methyl groups and a carbonyl), it does not appear clear what preferred binding geometry can be expected.

The benzene, toluene, *p*-xylene, and triphenylmethane substrates are found to act as guests with the cavity, where the K_{11} values clearly demonstrate that the relative bindings are weak. Due to steric consideration, one can easily rule out the Pd_3···π-(C=C) interactions. Therefore, hydrophobic and agostic interactions are solely responsible for the (weak) binding in these cases. The following experiment is concerned with the smaller benzene substrate where the starting geometry was set to be analogous to the benzoate; one of the H-atoms is positioned pointing down in the cavity. During the minimization process, the benzoate molecule rotates around its C_6 axis by 30° to allow two ortho-hydrogen atoms to lie flat on top of the Pd_3 plane. In this position, the steric interactions are provided by the methylene hydrogen (no. 3 and no. 6). A second experiment was also attempted where the benzene is now oriented at 90° with respect to the benzoate geometry of Figure 8, with one hydrogen atom pointing down in the cavity as well. After the computation, the benzene substrate rotated again by 30° around its C_6 axis as shown in Figure 9. The interesting feature here is that the benzene molecule lie in a quasi-sandwich structure between the dppm–phenyl groups nos. 1, 8, 4, and 5. The stacking occurs via intercalating C–H bonds. The intercarbon distances (between the phenyl groups; nos. 1 and 8 and nos. 4 and 5) are ~3.5–3.6 Å closer to the sum of van der Waals radii. The closest H···H contacts are slightly over 2 Å. Further attempts in pushing the benzene group deeper in the cavity resulted in a rapid increase in the calculated potential energy. One of the two H-atoms lies almost exactly above the Pd_3 center with distances approaching 2.4–2.5 Å. Knowing that the van der Waals radii for Pd is 1.6 Å, and 2.4–2.5-Å values represent a weak contact that allows theoretical intermolecular agostic interactions to take place if such a case occurs. The presence of spectroscopic changes and

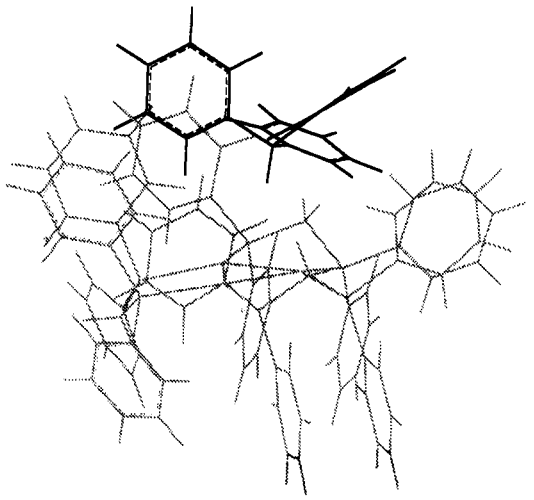

A

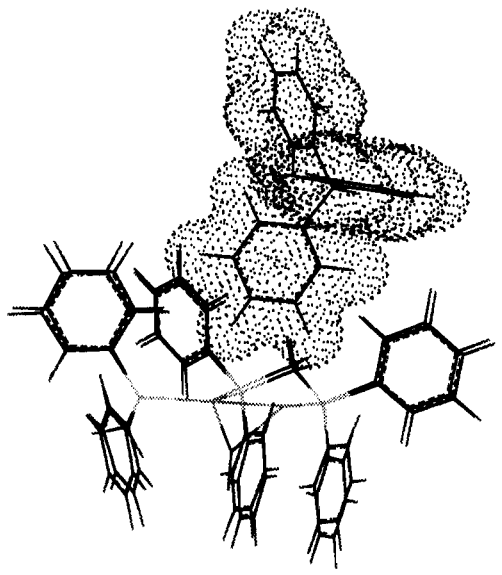

B

Figure 10. Minimized structures for triphenylmethane in the cavity via the methylene C–H bond (A) and via a phenyl group. In the first modeling experiment the smallest Pd–H distances was kept at 3 Å. In the second (B) experiment, the smallest Pr–H distances are kept at 3 Å. In the second (B) experiment, the smallest Pd–H distance is 2.4 Å.

isosbestic points as discussed in the previous section witness these interactions. On the basis of the low K_{11} values, the combination of *weak* agostic and hydrophobic interactions appears to be responsible for the binding in this case.

The modeling experiments for toluene (and *p*-xylene) depended upon how the molecules were set in the cavity prior to computations. In some occasions the methyl group was expelled from the cavity; in others, the methyl group remained in the cavity where the computed M···H distances were about 2.4 Å, again at distances favoring intermolecular agistic interactions. If such an event occurs, the C_{3v} symmetry of both the Pd_3 center and the methyl group could amplify these interactions by 3-fold.

The last modeling experiments involved the bulky triphenylmethane substrate. Attempts to place the methylene C–H bond in the cavity invariably led to the large distortion of the substrate (Figure 10) even at long Pd···H distances (~3.5 Å). On the other hand, setting the starting configuration with a phenyl group pointing in the cavity similar to the benzene substrate resulted in the minimization as expected, with the phenyl group adopting the quasi-sandwich structure as described for benzene. However, setting the shortest Pd···H distance to be ~2.5 causes the substrate to undergo some distortions (Figure 10) where the phenyl groups are slightly rotated. We come to the conclusion that the binding occurring between triphenylmethane and $Pd_3(dppm)_3CO^{2+}$ must be weaker than the benzene binding and does not occur via the methyl hydrogen.

Final Remarks

The ground-state guest–host chemistry of the $Pd_3(dppm)_3CO^{2+}$ cluster has now been described in some detail for a variety of substrates. The binding strength of a substrate (both organic and inorganic) into the cavity is found to be related to the charge, the ligand behavior (or strength), the size, and the hydrophobic (and agostic) properties of the substrates which is consistent with the bifunctional recognition properties of the cluster (metal cations and hydrophobic cavity). We have also noticed that the empty cavity compound in the solid state ($[Pd_3(dppm)_3CO](PF_6)_2$ and the weakly interacting cavity species (such as in the Pd_3···methanol case) exhibit the most red-shifted λ_{max} of absorption (~496 nm). As a result, the presence of a substrate in the cavity invariably leads to the appearance of a blue-shifted new band. The new λ_{max} is not the same for each substrate; the λ_{max} range is from 466 to 490 nm. The difference in λ_{max} values can be rationalized by the presence of Pd_3···substrate interactions, hence stabilizing the HOMO. In the cases where the Pd_3···substrate interactions are weak (such as benzene), the presence of the substrate in the cavity induces dppm conformational changes. The striking evidence is found in the X-ray results where the angles between the Pd_3–plane and the P atoms are far from linearity[10] in the $[Pd_3(dppm)_3CO](PF_6)_2$ salts with respect to the structure where the cavity is filled.[2] It is therefore suspected that the λ_{max} values are (mainly) related to the change in dppm conformation in these cases. Such large dppm conformational changes as shown in Figure 4 imply that the cavity somewhat loses *some* selectivity in terms of substrate sizes and orientational trajectory for the bindings. In many ways, the structural chemistry (stoichiometry and cavity–substrate orientation) resembles to some extent the one described for calixarene compounds[21a] and their recently reported metal complexes.[21b,c] Two major differences however predominate: (1) The calixarenes cannot accommodate more than one metal at the bottom of the cavity (lower rim), and (2) the benzyl groups in the calixarene ring exhibit a completely different degree of freedom (induced or not induced by the presence of a substrate in the cavity).[22]

Puddephatt et al.[2,4,5] pointed out that the $Pd_3(dppm)_3CO^{2+}$ cluster is (as the chemical formula states) an intereseting trimeric species as the triangular structure represents a good model for the surface structure for Pd(111). In this cluster, catalysis,[3] photoinduced C–H bonds and small-molecule activations,[23] must take place inside the cavity and, therefore must adopt the appropriate molecular arrangements prior to reactions. Therefore, this result has important consequences on the understanding of the mechanism by which these processes occur.

In the case of the $Pt_3(dppm)_3CO^{2+}$ analogue, the UV–visible spectra appear as a series of shoulders in the blue portion of the spectra. Spectroscopic changes upon addition of substrates are more difficult to monitor leading to large uncertainties in K_{11}. The Pt cluster was not investigated in this work. On the basis of the thermal chemistry elegantly established by Puddephatt *et al.*,[2a] the resemblance between Pd and Pt suggests that the guest–

(21) (a) Gutsche, C. D. *Calixarenes*; Thomas Graham House, Royal Society of Chemistry: London, U.K., 1989; and the references therein. (b) Corazza, F.; Floriani, C.; Chiesi-Villa, A.; Rizzoli, C. *Inorg. Chem.* **1991**, *30*, 4465. (c) Matt, D.; Loeber, C.; Vicens, J.; Asfari, Z. *J. Chem. Soc., Chem. Commun.* **1993**, 604.

(22) Conner, M.; Janout, V.; Regen, S. L. *J. Am. Chem. Soc.* **1991**, *113*, 9670.

(23) (a) Harvey, P. D.; Aye, K. T.; Provencher, R.; Socol, S. M. *Res. Trends.*, submitted for publication. (b) Harvey, P. D.; Lafontaine, M. Presented as a poster at the 198th National Meeting of the American Chemical Society, Boston, MA, April 15, 1990.

host chemistry should indeed be similar. Recent data on the flash photolysis and emission data analysis also demonstrated the presence of guest–host chemistry in the $Pt_3(dppm)_3CO^{2+}$ case.[14]

On the basis of recent molecular orbital calculations,[12,14,24] the lowest energy excited state is found to be M–M antibonding with respect to the ground state, and one could anticipate an increase in M···M separations and therefore in cavity size.[14] By analogy, this M···M bond weakening belongs to the same family that characterizes the $d\sigma \rightarrow d\sigma^*$ transitions in the d^7–d^7 and d^9–d^9 complexes,[25,26] leading to the formation of radical species. In the trinuclear clusters the odd electrons are delocalized in the M_3 molecular orbitals, and their photochemistry is unknown and should lead to yet to be discovered new photoinduced reactivity. Further research in this area is in progress.

Acknowledgment. This research was supported by the Natural Sciences and Engineering Research Council of Canada (NSERC) and the Fonds concerté pour l'avancement de la recherche (FCAR).

Supplementary Material Available: Tables giving crystal data and details of the structure determination, atomic coordinates, bond distances, bond angles, anisotropic thermal parameters, and hydrogen atom positions for $[Pd_3(dppm)_3CO](PF_6)_2$ and $[Pd_3(dppm)_3CO](CF_3CO_2)(PF_6)$ (30 pages). Ordering information is given on any current masthead page.

(24) (a) Mealli, C. *J. Am. Chem. Soc.* **1985**, *107*, 2245. (b) Evans, D. G. *J. Organomet. Chem.* **1988**, *352*, 397.
(25) Geoffroy, G. L.; Wrighton, M. S. *Organometallic Photochemistry*; Academic Press; New York, 1979.
(26) (a) Perreault, D.; Drouin, M.; Michel, A.; Harvey, P. D. *Inorg. Chem.* **1992**, *31*, 2740. (b) Metcalf, P. A.; Kubiack, C. P. *J. Am. Chem. Soc.* **1986**, *108*, 4682. (c) Reinking, M. K.; Kullberg, M. L.; Cutler, A. R.; Kubiak, C. P. *J. Am. Chem. Soc.* **1985**, *107*, 3517. (d) Yamamoto, Y.; Yamazaki, H. *Bull. Chem. Soc. Jpn.* **1985**, *58*, 1843.